Application of Flow Boiling for Thermal Management of Electronics in Microgravity and Reduced-Gravity Space Systems

Hui Zhang, Issam Mudawar, and Mohammad M. Hasan

***Abstract*—Large density differences between liquid and vapor create buoyancy effects in the presence of a gravitational field. Such effects can play an important role in two-phase fluid flow and heat transfer, especially critical heat flux (CHF). CHF poses significant risk to electronic devices, and the ability to predict its magnitude is crucial to both the safety and reliability of these devices. Variations in the gravitational field perpendicular to a flow boiling surface can take several forms, from flows at different orientations at $1g_e$ to the microgravity environment of planetary orbit, to the reduced gravity on the Moon and Mars, and the high g's encountered in fighter aircraft during fast aerial maneuvers. While high coolant velocities can combat the detrimental effects of reduced gravity, limited power budget in space systems imposes stringent constraints on coolant flow rate. Thus, the task of dissipating the heat must be accomplished with the lowest possible flow velocity while safely avoiding CHF. In this paper, flow-boiling CHF is investigated on Earth as well as in reduced gravity parabolic flight experiments using FC-72 as working fluid. CHF showed sensitivity to gravity at low velocities, with microgravity yielding significantly lower CHF values compared to those at $1g_e$. Differences in CHF value decreased with increasing flow velocity until a velocity limit was reached above which the effects of gravity became inconsequential. This proves existing data, correlations, and models developed from $1g_e$ studies can be employed with confidence to design reduced gravity thermal management systems, provided the flow velocity is maintained above this limit. This paper discusses two powerful predictive tools. The first, which consist of three dimensionless criteria, centers on determination of the velocity limit. The second is a theoretically based model for flow boiling CHF in reduced gravity below this velocity limit.**

***Index Terms*—Electronic cooling, microgravity, phase change.**

NOMENCLATURE

A	Cross-sectional area of channel.
b	Ratio of wetting front length to wavelength.
Bo	Bond number.
c_p	Specific heat.
D_h	Hydraulic diameter, 4 A/p.
Fr	Froude number.
g	Gravity.
g_e	Earth's gravity.
g_n	Component of gravity normal to heated surface.
$g_{//}$	Component of gravity opposite to direction of fluid flow.
H_f	Mean thickness of liquid layer.
h_{fg}	Latent heat of vaporization.
H_g	Mean Thickness of vapor layer.
L	Heated length.
P	Pressure.
p	Channel perimeter.
q''	Wall heat flux.
q''_m	Critical heat flux.
q''_w	Wetting front lift-off heat flux.
T	Temperature.
$\Delta T_{\mathrm{sub},o}$	Outlet subcooling, $T_{\mathrm{sat},o} - T_{b,o}$.
U	Mean liquid inlet velocity.
U_f	Mean velocity of liquid layer.
U_g	Mean velocity of vapor layer.
$U_{g,n}$	Mean vapor velocity in wetting front normal to heated surface.
U_∞	Bubble rise velocity.
We	Weber number.
z	Stream-wise coordinate.

Greek symbols

δ	Mean vapor layer thickness.
θ	Flow orientation angle.
λ_c	Critical wavelength.
ξ	Heat utility ratio.
ρ	Density.
ρ''_f	Modified liquid density.
ρ''_g	Modified vapor density.
σ	Surface tension.

Subscripts

c	Critical.
b	Bulk liquid.

Manuscript received April 03, 2008; revised July 11, 2008. First published January 09, 2009; current version published July 22, 2009. This work was supported by the National Aeronautics and Space Administration under Grant NNC04GA54G. This work was recommended for publication by Associate Editor T. Lee upon evaluation of the reviewers comments.

H. Zhang and I. Mudawar are with the Boiling and Two-Phase Flow Laboratory (BTPFL) and Purdue University International Electronic Cooling Alliance (PUIECA), West Lafayette, IN 47907-2088 USA (e-mail: mudawar@ecn.purdue.edu).

M. M. Hasan is with the NASA Glenn Research Center, Cleveland, OH 44135 USA.

Digital Object Identifier 10.1109/TCAPT.2008.2004413

f	Saturated liquid.
g	Saturated vapor.
i	Inlet to heated wall.
L	Based on heated length.
m	Maximum, critical heat flux.
o	Outlet from heated wall.
sat	Saturation.
sub	Subcooling.
w	Wetting front; heated wall.

I. Introduction

A. Importance of Two-Phase Thermal Management Systems to Future Space Missions

As SPACE missions increase in scope, size, complexity, and duration, so do both power and heat dissipation demands. This is particularly the case for future manned missions back to the Moon and afterwards to Mars. Paramount to the success of these missions is the ability to reduce the size and weight of all key thermal management subsystems. One means to achieve this goal is to reduce the surface area of heat exchange surfaces by replacing present mostly single-phase-based systems with two-phase systems. By capitalizing upon the merits of latent rather than sensible heat exchange, two-phase thermal management systems can yield orders of magnitude enhancement in evaporation and condensation heat transfer coefficients compared to single-phase systems. The potential improvements with the shift to two-phase systems are evident from several recent NASA workshops on power generation and life support systems [1]. These workshops have culminated in critical recommendations concerning the implementation of flow boiling and condensation for a variety of subsystems including Rankine cycle power generation, electronics cooling, cabin temperature control, space suit temperature regulation, waste management, and regenerative fuel cells.

B. Effects of Body Force on Critical Heat Flux (CHF)

Because of large density differences between liquid and vapor, buoyancy (which is proportional to the product of gravity and density difference) can play an important role in defining the motion of vapor relative to liquid and, therefore, influence heat transfer effectiveness. CHF is a prime example of a heat transfer phenomenon that can exhibit complex variations with gravity. It is of particular concern with heat-flux-controlled power and electronic devices, where it can lead to a sudden, unsteady rise in device temperature. Most devices are not designed to withstand such a temperature rise; hence, the device materials might melt, burn out, or undergo some other form of permanent damage. The challenge in designing a thermal management system for use in space is to make certain that the prevailing boiling heat flux is safely below CHF, hence the importance of predicting the precise conditions that trigger CHF. What makes this task especially challenging is that conventional means for enhancing CHF in a terrestrial environment (e.g., greatly increasing fluid flow rate and/or subcooling level) may not be permitted in a reduced gravity environment, given the large penalty in size, weight, and pumping power with such provisions.

Unfortunately, most of the two-phase flow and heat transfer know-how amassed over nearly a century of research comes from experiments that were conducted in Earth's gravity. Space missions, on the other hand, span varying gravitational levels as illustrated in Fig. 1. Microgravity is important to satellites and Earth-orbiting vehicles and stations. Future missions will require a strong understanding of the effects of reduced gravity ranging from Lunar to Martian levels. On the other side of the spectrum, two-phase systems onboard fighter aircraft must endure the high body forces associated with fast aerial maneuvers.

Interestingly, even at $1g_e$, the effects of buoyancy are by no means trivial. Take for example the simple configuration of saturated pool boiling. For a horizontal upward-facing heated surface, gravity points perpendicular to and towards the surface, and serves to remove vapor while replenishing the surface with bulk liquid. Howard and Mudawar [2] showed CHF mechanism is vastly altered as the surface is tilted away from horizontal. With a tilted surface, gravity can be broken into two components, one perpendicular to the surface, which pulls vapor away from the surface, and a second parallel to the surface, which induces vapor flow along the surface. As shown in Fig. 2, three distinct CHF mechanisms were observed. For surface inclinations between 0 and 60° away from normal, CHF follows the classical *Pool Boiling Regime* for vapor removal predicted by Zuber *et al.* [3]. Inclinations between 60 ° and 165 ° strengthen the component of gravity parallel to the surface, inducing vapor motion along the surface and resulting in a *Wavy Vapor Layer Regime*. Much larger inclinations, between 165 ° and 180 ° bring vapor above the denser liquid, resulting in a third *Stratification Regime*. Notice the slight reduction in CHF between 0 ° and 90 °, and the drastically reduced CHF at 180 °. The importance of these three CHF regimes to flow boiling CHF will become apparent later in this study.

The present study is the culmination of two NASA-sponsored efforts that are aimed to assess the role of gravity on flow boiling CHF. The first study was conducted at $1g_e$ at different flow orientations relative to gravity. In the second study, experiments were performed in parabolic flight to simulate microgravity as well as Lunar, Martian, and 1.8 g_e environments. Each of the two studies involved extensive high-speed video analysis of interfacial features as well as measurement of CHF data. In this paper, CHF mechanisms are identified, and a theoretical model is constructed for the dominant CHF mechanism in reduced gravity. Additionally, a method is developed to determine the minimum flow velocity that renders flow-boiling CHF insensitive to reduced gravity. This criterion allows existing knowledge of two-phase flow patterns and transitions, pressure drop, heat transfer, and CHF that has been amassed from $1g_e$ studies to be used with confidence to design two-phase systems for space missions.

Unlike the authors' prior studies, which explored the influence of various levels of body force on flow boiling CHF, the

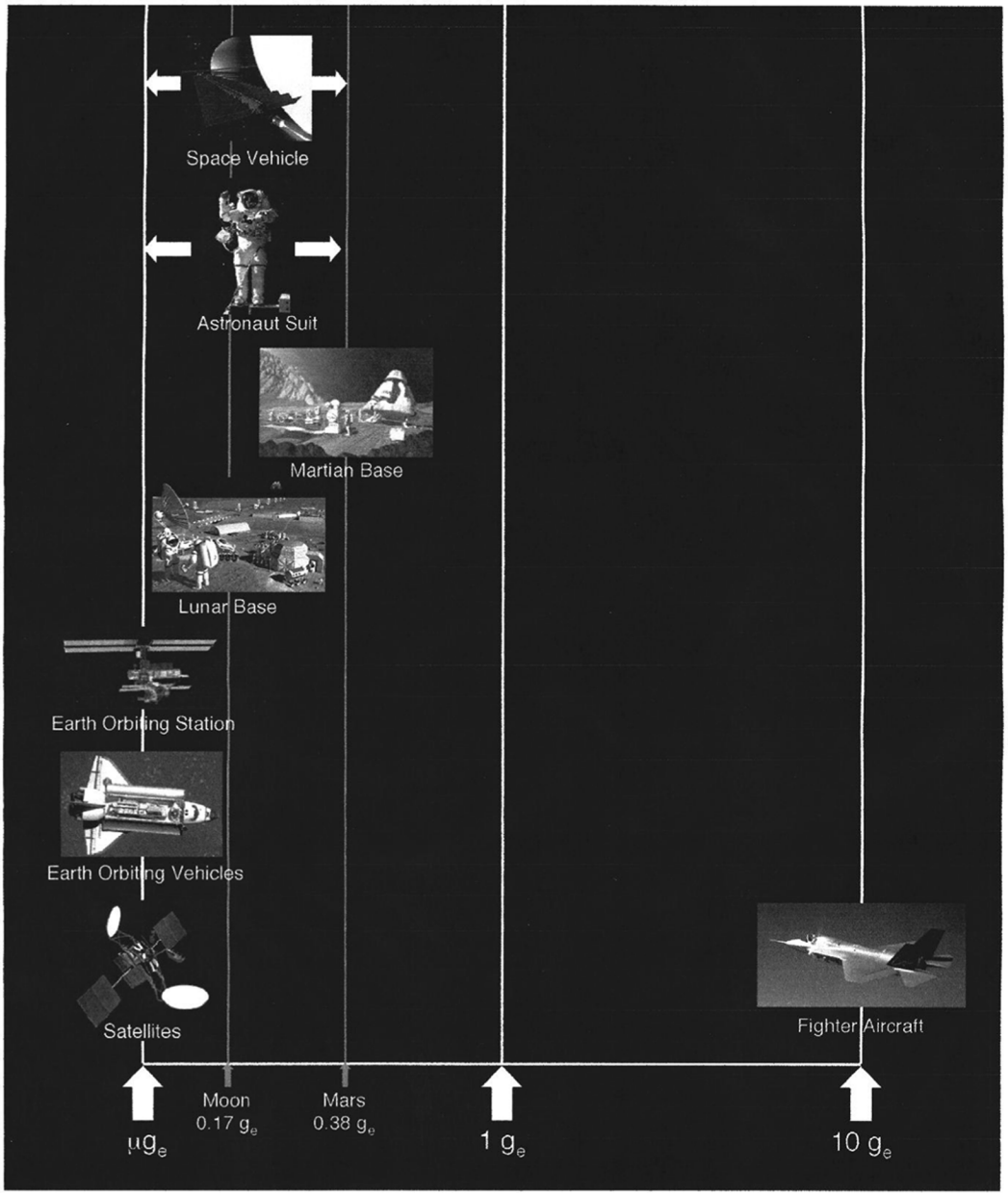

Fig. 1. Examples of systems demanding predictive models of the effects of gravitational field on two-phase flow and heat transfer.

present paper is the first attempt at consolidating experimental observations to develop theoretical models that can tackle a continuous range of body forces from microgravity to those encountered in military aircraft during fast aerial maneuvers.

II. Experimental Methods

A. *One-g_e Apparatus*

This first facility featured a flow boiling test module that could be tilted to any angle relative to Earth's gravity. This module was formed by clamping together two plates of transparent polycarbonate plastic. As shown in Fig. 3(a), the flow channel itself was formed by milling a 5.0 mm $\times$ 2.5 mm rectangular slot into the bottom plate of the test module. A heating block made from oxygen-free copper was flush-mounted along one side of the flow channel. The wetted heated wall consisted of the edge of the thin section of the heating block, which measured 101.6 mm long by 2.5 mm wide. The wetted wall was heated by supplying electrical power to cartridge heaters that were embedded in the thick section of the copper block. Five arrays of Type-K thermocouples were inserted along the thin section of the heating block. Each array consisted of three thermocouples situated 1.02, 6.10, and 11.18 mm from the wetted wall. A linear curve fit to the thermocouple readings in each array yielded a temperature gradient perpendicular to the wall that was used to calculate both local heat flux, q'', and local wall temperature T_w with 7.9% and 0.3 °C uncertainty, respectively. Fluid temperature and pressure were measured through taps in the cover plate both upstream and downstream of the heated wall. These measurements have uncertainties of 0.3°C and 0.01%, respectively. Throughout the $1g_e$ experiments, outlet pressure was maintained at 138 kPa (20 psia).

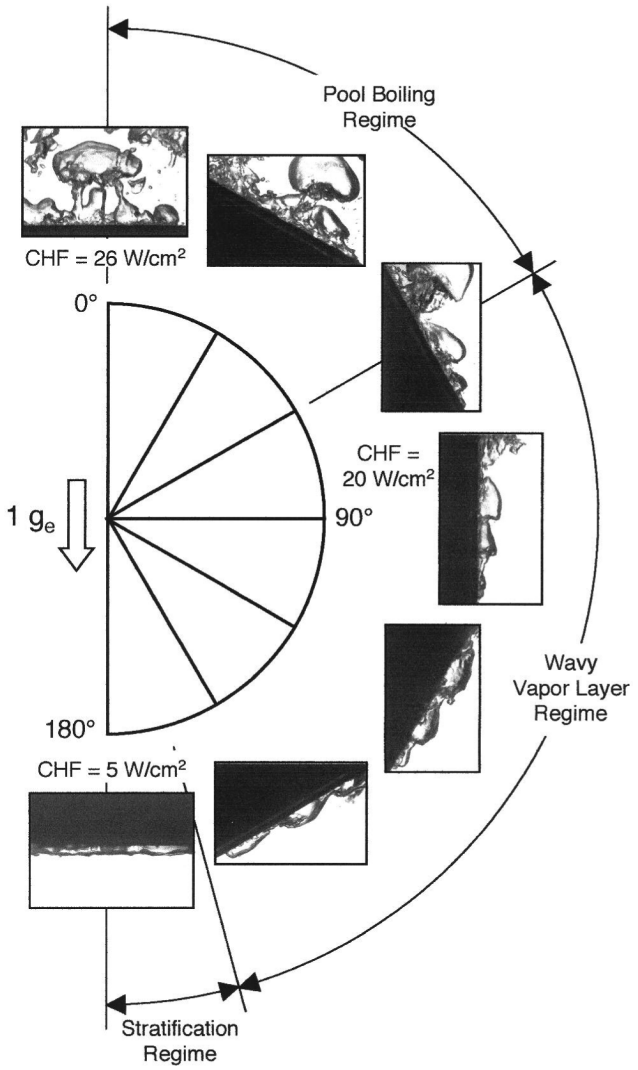

Fig. 2. CHF regimes for saturated pool boiling of PF-5052 from 1.27 cm × 1.27 cm heated surface at different orientations (adapted from Howard and Mudawar [2]).

Fig. 3(b) depicts the test module mounted on an angular translation platform atop a steel cart containing all components of the two-phase flow loop, in addition to instrumentation and power control panels. Fig. 3(c) shows the main components of a closed two-phase flow loop that was used to supply liquid FC-72 to the test module at desired operating conditions. Further details of this facility can be found elsewhere [4], [5].

B. Parabolic Flight Apparatus

Like the 1-g_e apparatus, the parabolic flight apparatus featured a flow-boiling module consisting of two transparent polycarbonate plastic plates and a heater assembly. As shown in Fig. 4(a), a 5.0 × 2.5 mm rectangular flow channel was milled into the underside of the top plastic plate. The heated wall consisted of a 0.56-mm-thick and 101.6-mm-long copper plate that was heated by a series of thick-film resistors. As shown in Fig. 4(b), the heater assembly consisted of six thick-film resistors that were soldered to the underside of the copper plate. The heater assembly featured fast temperature response to changes in heat flux and gravitational acceleration, which is crucial during flight experiments. With the small thickness of the copper plate and small thermal mass of the resistors, the wall temperature could reach steady state in less than 5 s following a heat flux increment. On the other hand, the 0.56-mm thickness of the copper plate was sufficiently large to preclude any CHF dependence on copper plate thickness [6]. Wall temperature was measured by five thermocouples inserted into the copper plate. These thermocouples had an uncertainty of 0.3 °C. The heat flux was determined by dividing electrical power input to the resistors by the wetted area of the heated wall. Overall uncertainty of the heat flux measurement was 0.2 W/cm ^{2}. Two additional thermocouples provided fluid temperature readings just upstream and downstream of the heated wall with an uncertainty of 0.3 °C. Pressure transducers at the same locations provided pressure readings with an accuracy of 0.01%. Outlet pressure in all the parabolic flight experiments was maintained at 1.44 bar (20.9 psia).

Fig. 4(c) shows a schematic diagram of the test loop that was used to both deaerate the working fluid, FC-72, prior to testing and maintain desired flow conditions during the tests. Aside from components similar to those employed in the 1-g_e flow loop, the flight loop used an accumulator charged with nitrogen gas to maintain fluid pressure downstream of the heated wall. The entire flight apparatus, including the flow loop components, power and instrumentation cabinets, and data acquisition system, was mounted onto a rigid extruded aluminum frame as shown in Fig. 4(d).

Reduced gravity was simulated aboard a plane that flew a series of parabolic maneuvers. Reduced gravity conditions, such as microgravity, Lunar gravity (0.16 g_e), and Martian gravity (0.38 g_e), were achieved with different parabolic maneuvers. A flight mission usually consisted of four sets of ten parabolas with about 5-min break between consecutive sets. Ten flight missions, about 450 parabolas, were dedicated to the present study aboard two different aircraft, NASA's KC-135 turbojet and Zero-G Corporation's Boeing 727-200. During a parabolic flight experiment, the desired fluid flow conditions were set before each set of parabolas. Power to the heater assembly was set and maintained before pulling out from a 23-s microgravity period. The power was then increased in increments of 1 to 3 W/cm^2 until a sudden unsteady rise in wall temperature was detected during a microgravity period. Flow boiling CHF is defined as the last heat flux measured prior to the unsteady temperature rise. Besides measuring CHF, vapor behavior was monitored near the outlet of the heated wall with the aid of a high-speed video camera. Further details of this facility can be found elsewhere [6], [7].

III. Experimental Results

A. One-g_e Results

For the 1-g_e experiments, the flow-boiling module was mounted on a rotation stage that enabled testing at different orientations relative to Earth's gravity. Tests were performed at orientations ranging from $\theta = 0°$, corresponding to horizontal flow with the heated surface facing upwards, and increasing counterclockwise in 45° increments. Notice how Earth's gravity is perpendicular to the heated surface for $\theta = 0°$

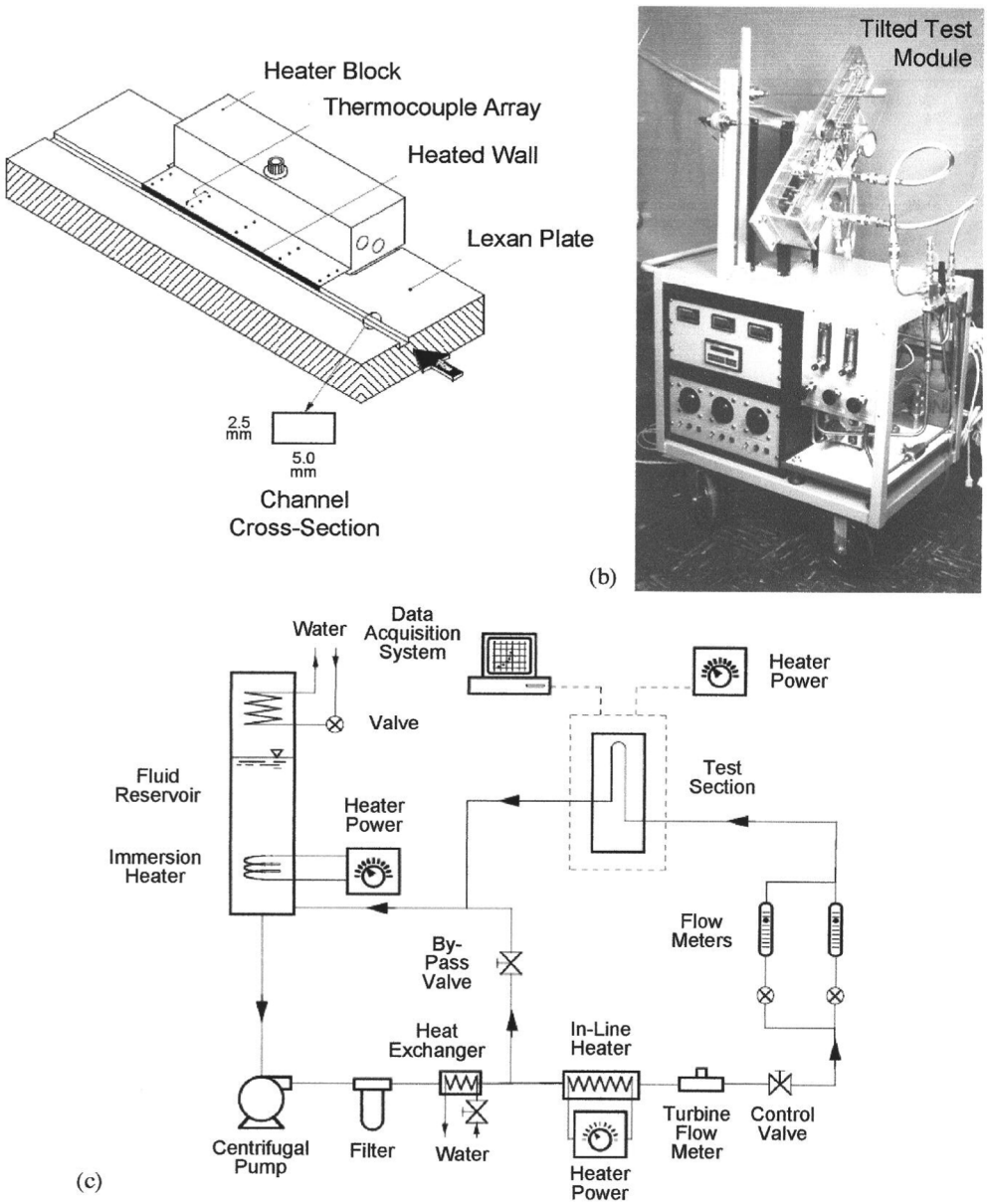

Fig. 3. 1 g_e apparatus. (a) Heater inserted into bottom plate of test module. (b) Photo of apparatus. (b) Schematic of two-phase flow loop.

(similar to pool boiling from a horizontal surface), and parallel but opposite to the liquid flow for $\theta = 90°$ (vertical upflow).

Fig. 5(a) shows vapor behavior at CHF-(conditions just preceding CHF) for near-saturated flow ($\Delta T_{\mathrm{sub},o} = 3$ °C) at a relatively low inlet velocity of $U = 0.1$ m/s. Because of strong buoyancy effects compared to liquid drag, orientation has significant influence on the CHF mechanism. Shown are four drastically different CHF regimes: 1) *Pool-Boiling Regime* for $\theta = 0°$, 2) *Wavy Vapor Layer Regime* for $\theta = 90°$, 3) *Stratified Regime* for $\theta = 180°$, and 4) *Vapor Stagnation Regime* for $\theta = 270°$. Notice that, because of the low flow velocity, the first three CHF regimes correspond very closely with the pool boiling regimes observed by Howard and Mudawar [2] and depicted in Fig. 2.

In the Pool Boiling Regime ($\theta = 0°$), bubbles coalesce on the heated surface before being detached by buoyancy and driven into the liquid core with minimal tendency to flow with the liquid. The Wavy Vapor Layer Regime ($\theta = 90°$) is the result of bubble coalescence into vapor patches that propagate along the heated surface mimicking a continuous vapor layer. Cooling of the surface appears to take place between the vapor patches, where liquid is able to contact the surface. The Stratification Regime ($\theta = 180°$) occurs when vapor resides above the liquid in the form of a thick, fairly smooth layer covering nearly the entire heated surface. The Vapor Stagnation Regime ($\theta = 270°$) is the result of a balance between buoyancy force and the drag force exerted by the liquid on the vapor. Two additional CHF regimes were observed at low flow velocities. A *Separated Concurrent Vapor Flow Regime* occurred at velocities slightly greater than $U = 0.1$ m/s, when liquid drag exceeded buoyancy. Conversely, a *Vapor Counter Flow Regime* was detected at velocities below 0.1 m/s, when buoyancy exceeded liquid drag and was therefore able to push vapor backwards towards the channel inlet. Aside from the drastic differ-

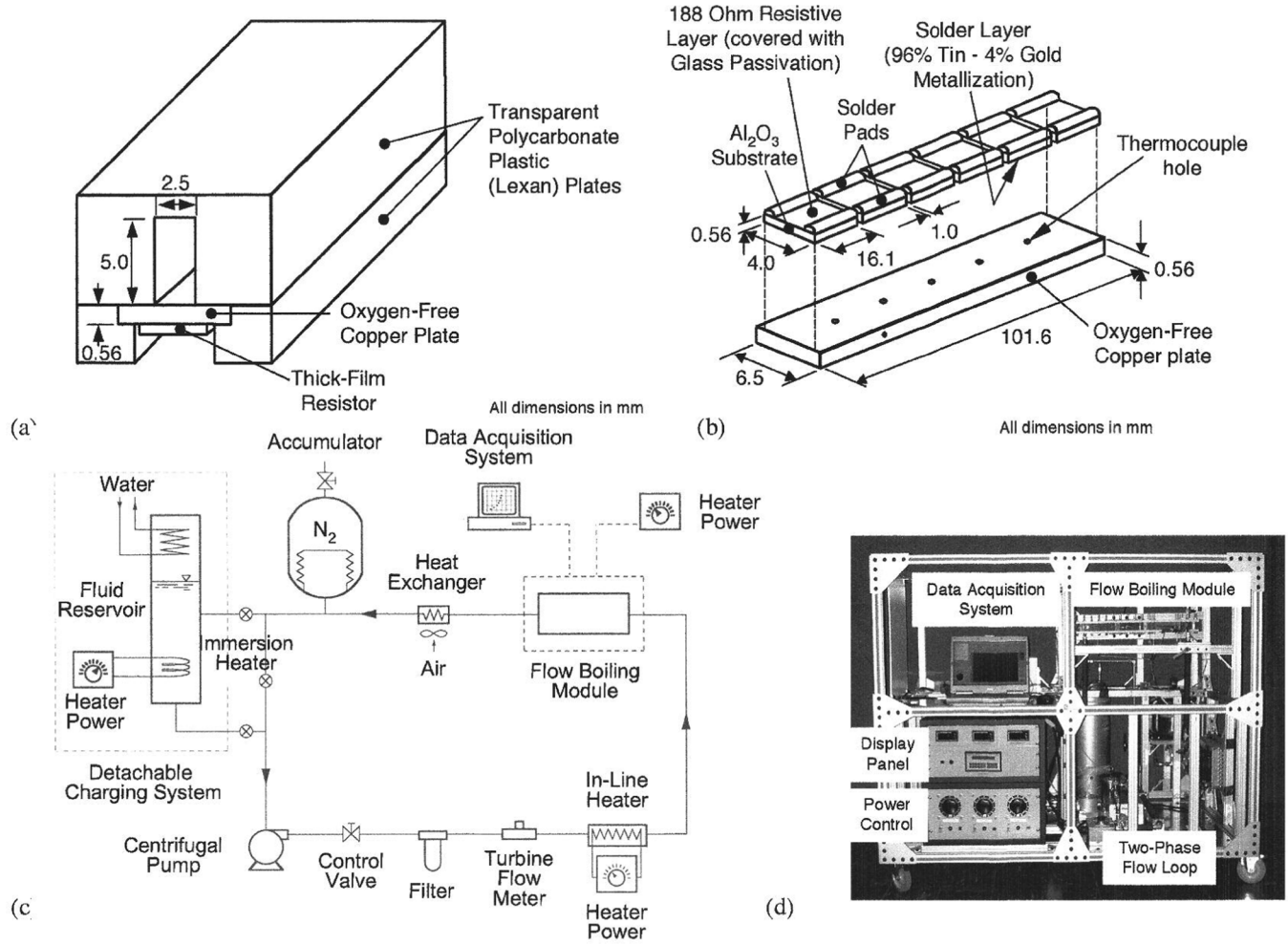

Fig. 4. (a) Flow channel assembly. (b) Heated wall construction. (c) Two-phase loop schematic. (d) Photo of parabolic flight apparatus.

ences in vapor behavior, notice the large differences in CHF magnitude among the four orientations.

Fig. 5(b) depicts vapor behavior for near-saturated flow ($\Delta T_{\text{sub},o} = 3\ ^\circ\text{C}$) at a relatively high velocity of $U = 1.5$ m/s. Large drag forces in this cause dwarf any buoyancy effects, virtually eliminating the effects of orientation, evidenced by the same Wavy Vapor Layer Regime dominating all orientations and fairly equal CHF values for all orientations. Overall, these observations are consistent with previous flow orientation studies by Simoneau and Simon [8], Mishima and Nishihara [9], and Gersey and Mudawar [10], [11].

B. Parabolic Flight μg_e Results

In microgravity, buoyancy becomes too weak to detach bubbles away from the heated surface. Surface tension tends to keep coalescent bubbles on the surface, while liquid drag causes the vapor to propagate along the surface. Therefore, there are fundamental differences between low velocity flow boiling behaviors at $1g_e$ and μg_e.

Unlike the $1 - g_e$ vapor behavior discussed in the previous section, Fig. 6 shows *flow-boiling CHF in μg_e follows the same mechanism at both low and high velocities*. For near-saturated flow at both $U = 0.25$ m/s and $U = 1.4$ m/s, bubbles coalesced along the heated wall into fairly large vapor patches in accordance with the Wavy Vapor Layer Regime. Fig. 6(c) shows similar CHF behavior at $U = 0.14$ m/s and a relatively highly subcooling of 22.8 °C.

To better understand the trigger mechanism for CHF in the Wavy Vapor Layer Regime, a few μg_e experiments were performed at $U = 0.15$ m/s and $\Delta T_{\text{sub},o} = 3\ ^\circ\text{C}$, in which high-speed video imaging captured interfacial behavior during the CHF transient. Fig. 7(a) shows, just before CHF, vapor patches grew into a wavy vapor layer that propagated along the wall as vigorous boiling in wetting fronts between the vapor patches provided the main mode for heat transfer from the heated surface to the liquid. Notice the downstream wetting front in Fig. 7(b) beginning to lift off from the heated surface as the CHF transient progressed. This lift-off triggered a chain reaction in which upstream wettings fronts began to detach from the surface, Fig. 7(c), until the entire heated surface was engulfed in a continuous insulating wavy vapor layer. This behavior is consistent with the Interfacial Lift-off CHF Model proposed by Galloway and Mudawar [12], [13] and Zhang *et al.* [5].

The differences in vapor behavior between $1g_e$ and μg_e observed in the present study are fairly consistent with those of

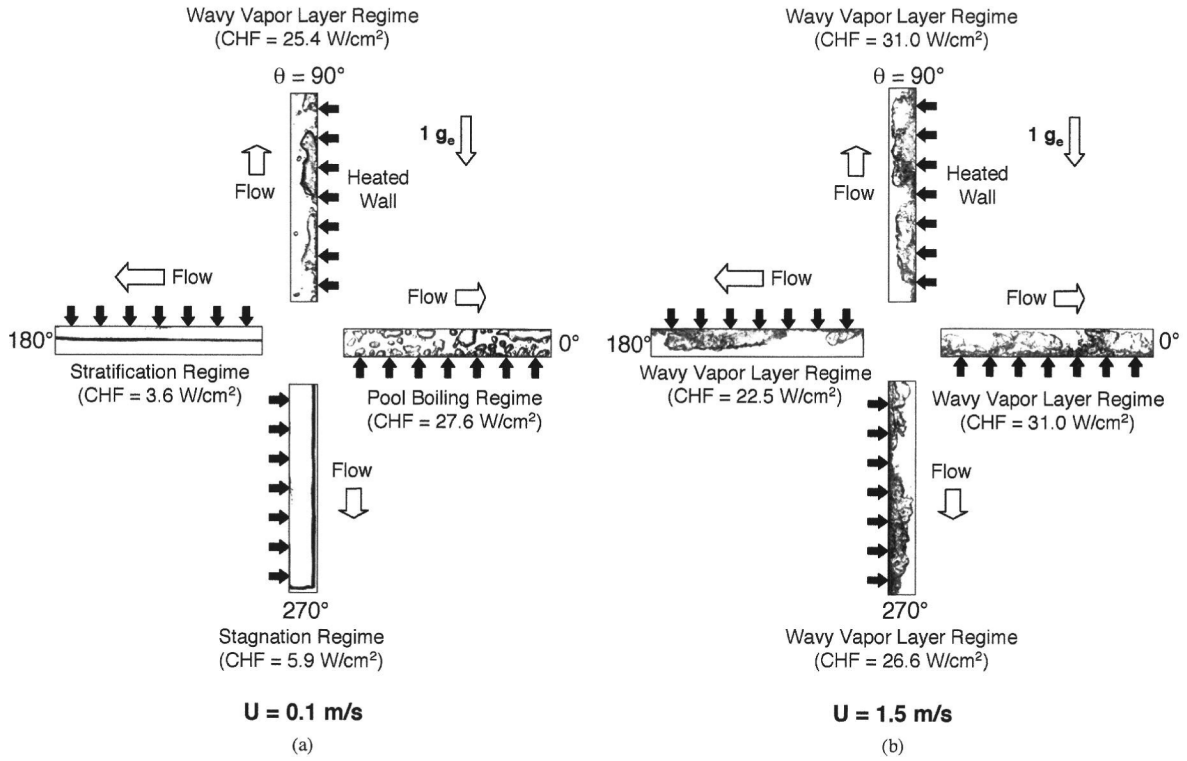

Fig. 5. Near saturated flow boiling CHF regimes at 1 g_e corresponding to different flow orientations for (a) $U = 0.1$ m/s and (b) $U = 1.5$ m/s. CHF regime and magnitude are highly dependent on orientation for the lower velocity and independent of orientation for the higher velocity.

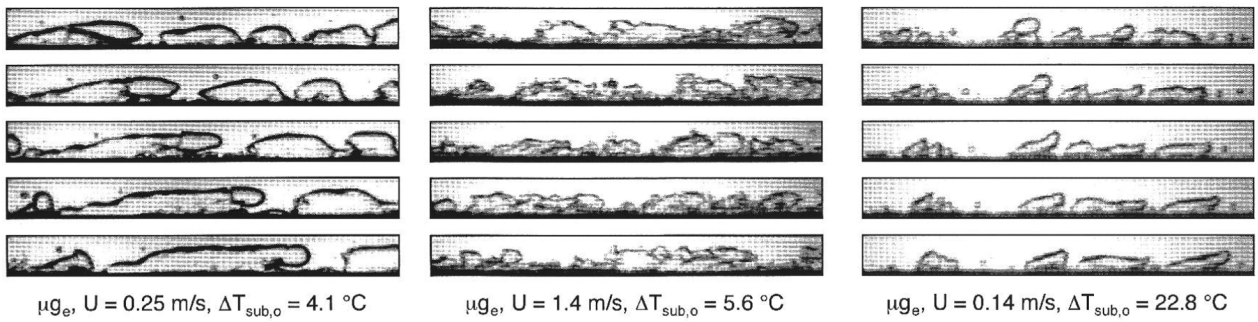

Fig. 6. Wavy Vapor Layer CHF Regime prevalent in μg_e at both low and high velocities as well as near-saturated and subcooled conditions.

prior μg_e studies. Saito *et al.* [14] also observed large differences in bubble behavior on the surface of a horizontal heated rod in $1g_e$ and μg_e. At $1g_e$, buoyancy helped bubbles detach from the rod surface very frequently. In the absence of buoyancy in μg_e, small bubbles coalesced into much larger ones along the heater rod and surrounded the heater rod downstream. Differences in vapor behavior between the two gravitational environments were more pronounced at lower velocities, higher heat fluxes and lower liquid subcooling. Cochran [15] observed bubbles in microgravity slid along the heated wall and coalesced into larger vapor masses rather than detached into the bulk flow. Ma and Chung [16] investigated flow boiling of FC-72 on a thin gold-film semitransparent heater at $1g_e$ and μg_e. They showed high velocities greatly reduce the influence of buoyancy, resulting in similar vapor behavior in both environments. They also observed a significant decrease in flow boiling CHF in μg_e compared with that in $1g_e$, but those differences decreased with increasing flow velocity [17].

C. Parabolic Flight 1.8 g_e Results

Fig. 8 depicts sequential images of flow boiling at low velocities and 1.8 g_e. Because of the high buoyancy force perpendicular to the heated surface, bubbles appear to be removed from the surface before they have the opportunity to coalesce, and boiling behavior seems to mimic pool boiling at $1g_e$. Fig. 8(b) shows high subcooling serves to quickly reduce the size of vapor bubbles during growth and detachment at the surface due to strong condensation effects.

D. Comparison of CHF Data for $1g_e$ and μg_e

Fig. 9 shows the variation of CHF with inlet liquid velocity at $1g_e$ and μg_e. In μg_e, the Wavy Vapor Layer Regime domi-

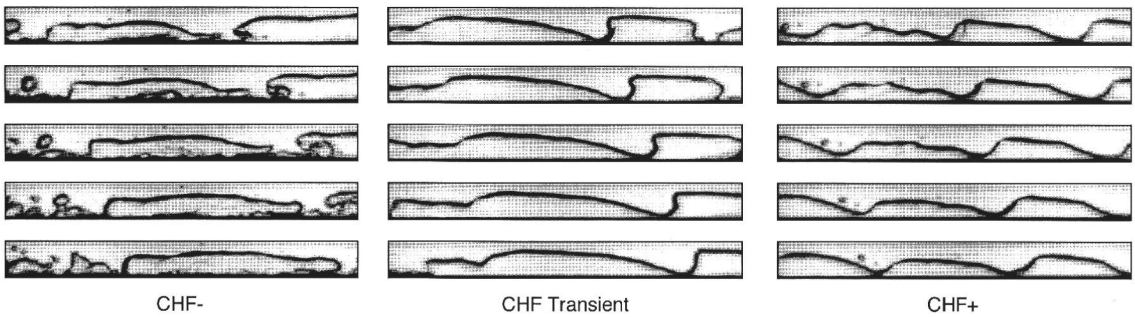

Fig. 7. CHF transient in μg_e for $U = 0.15$ m/s and $\Delta T_{\mathrm{sub},o} = 3.0$ °C.

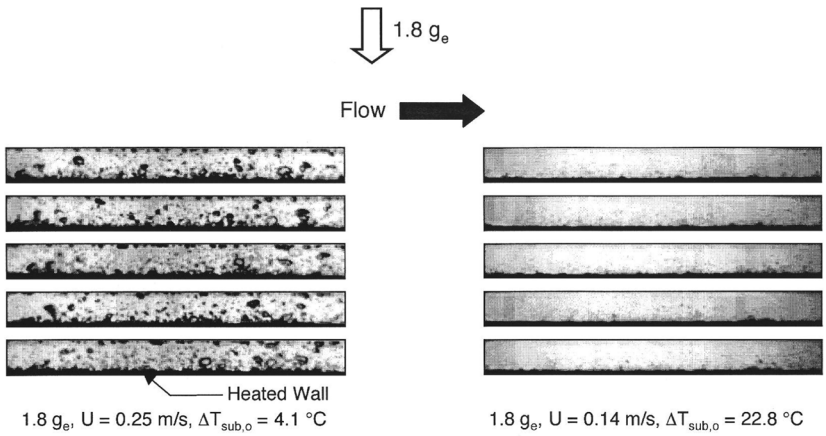

Fig. 8. Pool-boiling-like flow boiling at $1.8 g_e$.

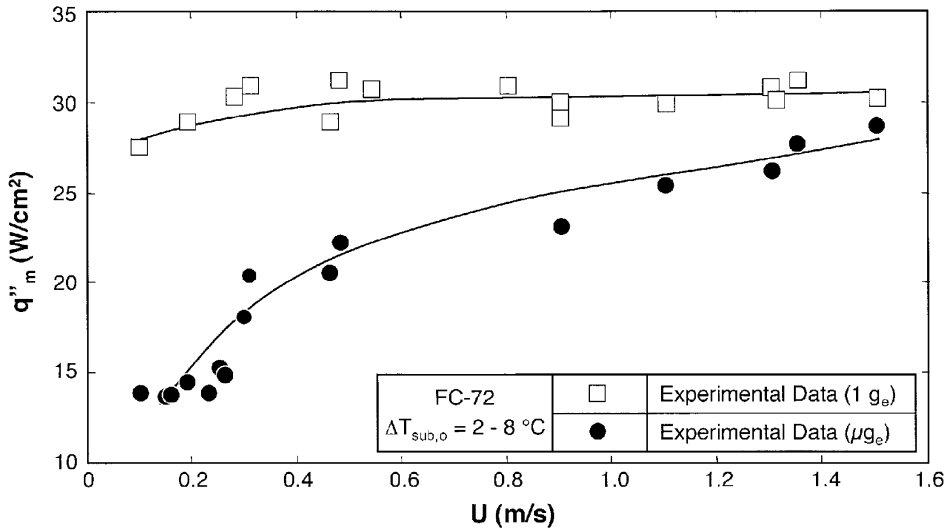

Fig. 9. CHF data for μg_e and horizontal $1 g_e$ flow boiling.

nates the entire velocity range, and CHF increases appreciably with increasing velocity because of the increased resistance to wetting front lift-off. In 1-g_e with the buoyancy force perpendicular to the surface, CHF follows the Pool Boiling Regime at low velocities and the Wavy Vapor Layer Regime at high velocities. Overall, the effect of velocity on CHF in $1 g_e$ is relatively mild. Notice how CHF at the lowest velocity in μg_e is only 50% of that in $1 g_e$. Increasing velocity helps reduce the influence of buoyancy force for the 1-g_e data and result in the same Wavy Vapor Layer Regime for both gravitational environments. The effects of buoyancy at $1 g_e$ become negligible around 1.5 m/s at which CHF values for $1 g_e$ and μg_e appear to converge.

The convergence of CHF data for both gravitational environments has important practical implications to the design of space thermal management systems. Knowing the velocity at which such convergence occurs allows designers to utilize the vast knowledge amassed from celestial two-phase studies (e.g., two-phase flow patterns and transitions, pressure drop, heat transfer,

CHF) to design reduced gravity thermal management systems with confidence, provided the liquid velocity exceeds the convergent value.

IV. Analysis

In this section, two design tools are introduced that enable thermal management system designers to tackle the complexities of flow boiling CHF in reduced gravity. The first is the theoretical Interfacial Lift-off CHF Model, which has been previously validated for 1-g_e pool boiling [2], 1-g_e flow boiling [[10]–[13], [18], [19]], and μg_e flow boiling [4], [5]. Unlike the original model, which is intended only for near-saturated flow, a technique is presented to extend the model to subcooled reduced gravity flows as well. The second tool is a set of dimensionless criteria that determine the minimum (convergent) velocity above which flow boiling CHF becomes "gravity-insensitive."

A. Modified Interfacial Lift-off CHF Model

As discussed earlier, the Interfacial Lift-off Model is based on the premise that flow-boiling CHF in the Wavy Vapor Layer Regime is triggered by separation of wetting fronts from the heated surface. Applying mass, momentum, and energy conservation to a differential control volume of the flow channel of length Δz enables the determination of mean liquid layer velocity U_f, mean vapor layer velocity U_g, and mean thickness δ of the vapor layer. These parameters are then used to determine the wavelength of the vapor-liquid interface according to the Helmholtz instability [13].

$$\frac{2\pi}{\lambda_c} = \frac{\rho_f'' \rho_g'' (U_g - U_f)^2}{2\sigma(\rho_f'' + \rho_g'')} + \sqrt{\left[\frac{\rho_f'' \rho_g'' (U_g - U_f)^2}{2\sigma(\rho_f'' + \rho_{g,''})}\right]^2 + \frac{(\rho_f - \rho_g) g_n}{\sigma}} \quad (1)$$

where g_n is the component of gravity perpendicular to the heated surface, $\rho_f'' = \rho_f \coth(2\pi H_f/\lambda_c)$, and $\rho_g'' = \rho_g \coth(2\pi H_g/\lambda_c)$.

Lift-off of the wetting front is assumed to occur when the momentum of vapor produced in the wetting front just exceed the pressure force associated with interfacial curvature; the latter tends to maintain interfacial contact with the heated surface. Using the sinusoidal shape of the interface given by (1), the mean pressure difference across the length $b\lambda_c$ of the wetting front ($b = 0.20$ from photographic analysis) is given by

$$\overline{P_f - P_g} = \frac{4\pi\,\sigma\,\delta}{b\,\lambda_c^2}\sin(\pi b). \quad (2)$$

At the moment of lift-off, the heat flux q_w'' concentrated in the wetting front is consumed by converting a mass of liquid into vapor whose momentum perpendicular to the heated surface $\rho_g u_{g,n}^2$ must just exceed the pressure difference given by (2). This condition can be expressed as

$$q_w'' = \rho_g(h_{fg} + c_{p.f}\Delta T_{\mathrm{sub},o})\left(\frac{\overline{P_f - P_s}}{\rho_g}\right)^{1/2} = \rho_g(h_{fg} + c_{p.f.}\Delta T_{\mathrm{sub},\alpha})\left[\frac{4\pi\sigma\delta}{\rho_g b\lambda_c^2}\sin(\pi b)\right]^{1/2}. \quad (3)$$

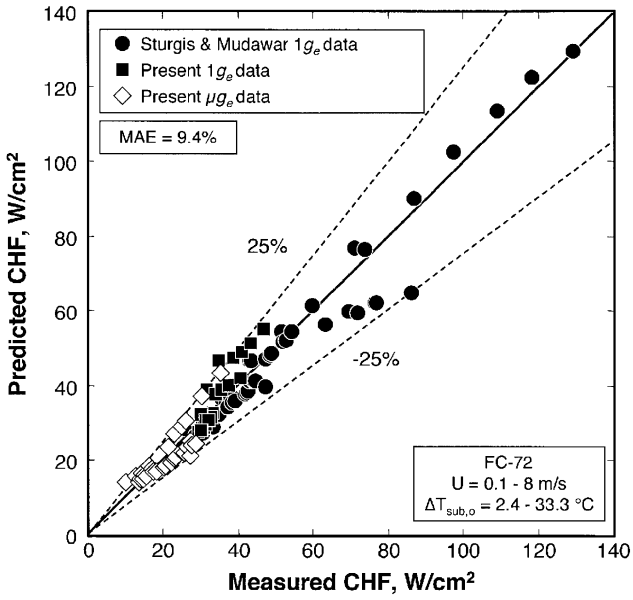

Fig. 10. Comparison of model predictions and CHF data measured at $1g_e$ and μg_e.

The heat flux given by (3) can be related to the value of CHF, q_m'', by $\xi\, q_m'' = b\, q_w''$, where ξ (termed *heat utility ratio*) is the portion of q_m'' at CHF that is dedicated to vapor generation. Therefore, CHF may be expressed as

$$q_m'' = \frac{b}{\xi}\rho_g(h_{fg} + c_{p.f.}\Delta T_{\mathrm{sub},o})\left[\frac{4\pi\sigma\delta}{\rho_g b\lambda_c^2}\sin(\pi b)\right]^{1/2}. \quad (4)$$

Additional details concerning the use of this equation and axial location for determining δ and λ_c is available in [6].

The difficulty in using (4) to determine CHF stems from a lack of theoretical understanding of the illusive parameter ξ. This parameter must satisfy the criteria $0 \le \xi \le 1$ for subcooled flow and $\xi = 1$ for saturated flow. A dimensionless relation that satisfies both criteria was derived from data obtained in the present study as well as a fairly extensive 1-g_e database for flow boiling CHF in a horizontal channel by Sturgis and Mudawar [18], [19]. Minimizing mean absolute error (MAE) in CHF prediction using the Interfacial Lift-off Model yielded the following heat utility relation:

$$\xi = 1 - \frac{\rho_f}{\rho_g}\frac{c_{pf}\,\Delta T_{\mathrm{sub},o}}{h_{fg}}\left[0.00285\left(\frac{\rho_f U^2 D}{\sigma}\right)^{0.2}\right]. \quad (5)$$

Fig. 10 shows the present model is successful at predicting the present μg_e and 1-g_e CHF data as well as the 1-g_e data of Stugis and Mudawar. Virtually all the data fall within $\pm 25\%$ of the model predictions, and the MAE for the combined database is 9.4%.

B. Minimum Velocity for Gravity-Insensitive Flow Boiling

As discussed earlier, it is possible to design "gravity-insensitive" reduced-gravity systems by maintaining flow velocity above the convergence value for 1-g_e and μg_e CHF data. Such systems allow data, correlations, and models developed on Earth to be safely implemented in space system design. The approach

adopted here in developing minimum (convergent) velocity criteria is to examine the 1-g_e CHF data and determine conditions under which the effects of gravity can be ignored.

In general, gravity can be decomposed into two components, one perpendicular, and the other parallel to, the surface. The component perpendicular to the surface influences hydrodynamic instability of the vapor-liquid interface. The critical wavelength, λ_c, of Helmholtz instability given by (1) can be rearranged into the form

$$\frac{2\pi}{\lambda_c}\frac{\sigma(\rho_f+\rho_g)}{\rho_f\rho_g(U_g-U_f)^2} = \frac{1}{2}\left\{1+\sqrt{1+4\frac{(\rho_f-\rho_g)(\rho_f+\rho_g)^2\sigma g_n}{\rho_f^2\rho_g^2(U_g-U_f)^4}}\right\} \quad (6)$$

The right-hand side of (6) approaches unity when the component of body force perpendicular to the heated surface is too weak to influence interfacial instability. This condition can be expressed as

$$\left|\frac{(\rho_f-\rho_g)(\rho_f+\rho_g)^2\sigma g_n}{\rho_f^2\rho_g^2(U_g-U_f)^4}\right| \ll \frac{1}{4}. \quad (7)$$

This criterion was examined by substituting the phase velocity difference by the characteristic flow velocity U of the flow channel. The dimensionless group in (7) can also be expressed as $\mathrm{Bo}/\mathrm{We}^2$, where Bo and We are the Bond and Weber numbers, respectively, which are defined as

$$\mathrm{We} = \frac{\rho_f\rho_g U^2 L}{(\rho_f+\rho_g)\sigma} \quad (8)$$

and

$$\mathrm{Bo} = \frac{(\rho_f-\rho_g)g_n L^2}{\sigma}. \quad (9)$$

Since the 1-g_e data showed insensitivity to orientation for $U = 1.5$ m/s or greater, the magnitude of $\mathrm{Bo}/\mathrm{We}^2$ for $U = 1.5$ m/s is used as a criterion for the gravity insensitive CHF regime

$$\frac{\mathrm{Bo}}{\mathrm{We}^2} = \frac{(\rho_f-\rho_g)(\rho_f+\rho_g)^2\sigma g_e}{\rho_f^2\rho_g^2U^4} \le 0.09. \quad (10)$$

The second component of gravity that influences flow boiling CHF at $1g_e$ is the component along the direction of (or opposite to) the liquid flow. This is the component responsible for the aforementioned Separated Concurrent Vapor Flow Regime, Vapor Stagnation Regime, and Vapor Counter Flow Regime. The latter two regimes are especially troubling because they yield unusually low CHF values. Besides, the Vapor Counter Flow Regime can interrupt the liquid flow and lead to flooding. Vapor flow in both of these regimes took the form of a long slug bubble whose velocity relative to liquid can be expressed as [20]

$$U_\infty = 0.35\,\frac{[(\rho_f-\rho_g)g_{//}D_h]^{1/2}}{\rho_f^{1/2}}. \quad (11)$$

Vapor Stagnation occurs when $U_\infty = U$, and counterflow when $U_\infty > U$. Both CHF regimes may be avoided when $U_\infty \ll U$,

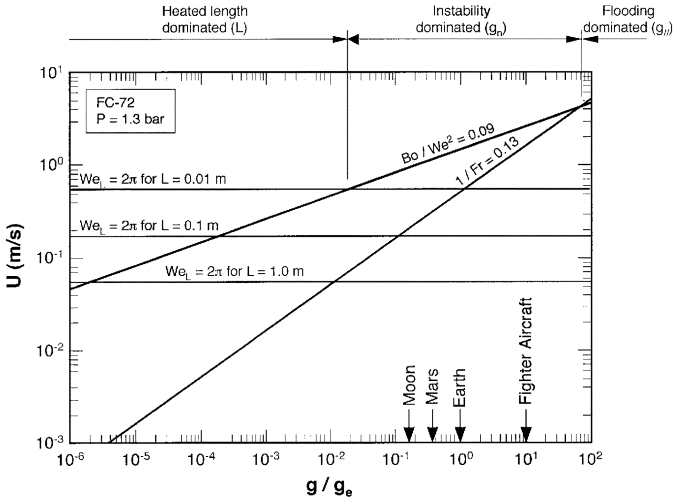

Fig. 11. Determination of minimum flow velocity required to overcome all body force effects on flow boiling CHF.

which, after replacing $g_{//}$ with g_e, can be represented in terms of the Froude number as

$$\frac{1}{\mathrm{Fr}} = \left|\frac{(\rho_f-\rho_g)g_e D_h}{\rho_f U^2}\right| \ll 8.16. \quad (12)$$

Since vapor counterflow and vapor stagnation ceased to exist for $U > 0.5$ m/s [4], this value was substituted in (12) yielding $1/\mathrm{Fr} = 0.13$. Therefore, a sufficient criterion for avoiding both detrimental CHF regimes can be expressed as

$$\frac{1}{\mathrm{Fr}} = \frac{(\rho_f-\rho_g)g_e D_h}{\rho_f U^2} \le 0.13. \quad (13)$$

A third criterion for minimum velocity concerns the wavelength of the Helmholtz instability. In particular, low flow velocities were found to produce a very large wavelength [6]. Therefore, a single vapor patch may cover the entire length L of the heated surface. The criterion $\lambda_c < L$ (where λ_c is given by (1)) can be expressed in the following Weber number form:

$$\mathrm{We}_L = \frac{\rho_f\rho_g U^2 L}{(\rho_f+\rho_g)\sigma} \ge 2\pi. \quad (14)$$

The three criteria given by (10), (13), and (14) can be used collectively to identify operating conditions that negate the influence of gravity on flow boiling CHF. Fig. 11 shows the minimum velocity required to satisfy the above criteria as a function of g/g_e. Each of the above three criteria predicts a particular value of U that must be exceeded in order to overcome body force effects. Since these criteria must be satisfied simultaneously, exceeding the largest of the three values becomes the determining criterion. Fig. 11 shows the minimum velocity for Earth, Martian, and Lunar environments is dominated by the instability criterion, while μg_e conditions may be influenced by the heated length criterion, especially for short heated surfaces.

V. Conclusion

In this paper, flow boiling CHF experiments were performed in an inclined channel at $1g_e$ as well as in reduced gravity parabolic flight. Photographic studies of the vapor-liquid interface were used to identify the dominant CHF mechanism in each environment. Theoretical models are presented to aid the designer of a two-phase thermal management system in avoiding this important catastrophic limit. Key findings from the study are as follows.

1) Several complex CHF regimes were identified for flow boiling in inclined channels at $1g_e$. All but one regime, the Wavy Vapor Layer Regime, are the result of the strong influence of buoyancy on vapor behavior. The Wavy Vapor Layer Regime, which is encountered at all velocities in vertical upflow and relatively high velocities in all orientations, shows virtually no sensitivity to orientation above a certain velocity limit.
2) Unlike 1-g_e flow boiling, only the Wavy Vapor Layer Regime was observed in μg_e. CHF values for this environment at low velocities are significantly smaller than in horizontal flow at $1g_e$. CHF differences between the two environments decrease with increasing velocity, culminating in virtual convergence above a certain velocity limit. This proves existing data, correlations, and models developed from 1-g_e studies can be employed with confidence in designing reduced gravity thermal management systems, provided flow velocity is maintained above this limit.
3) Three dimensionless criteria were developed to determine the minimum flow velocity required to overcome the effects of gravity on flow boiling CHF. Depending on the magnitude of gravity, working fluid, operating conditions, and length of heated surface, this limit is dictated by hydrodynamic instability, flooding, or length criteria.
4) For low velocity conditions where CHF is sensitive to gravity, the Interfacial Lift-off Model is a very effective tool for predicting flow-boiling CHF in both $1g_e$ and μg_e as well as saturated and subcooled flows.

References

[1] F. P. Chiaramonte and J. A. Joshi, "Workshop on Critical Issues in Microgravity Fluids, Transport, and Reaction Processes in Advanced Human Support Technology—Final Report," NASA TM-2004-212940, 2004.

[2] A. H. Howard and I. Mudawar, "Orientation effects on pool boiling CHF and modeling of CHF for near-vertical surfaces," *Int. J. Heat Mass Transfer*, vol. 42, pp. 1665–1688, 1999.

[3] N. Zuber, M. Tribus, and J. W. Westwater, "The hydrodynamic crisis in pool boiling of saturated and subcooled liquids," in *Proc. Int. Developments in Heat Transfer: Proc. Int. Heat Transfer Conf.*, Boulder, CO, 1961, pp. 230–236.

[4] H. Zhang, I. Mudawar, and M. M. Hasan, "Experimental assessment of the effects of body force, surface tension force, and inertia on flow boiling CHF," *Int. J. Heat Mass Transfer*, vol. 45, pp. 4079–4095, 2002.

[5] H. Zhang, I. Mudawar, and M. M. Hasan, "Experimental and theoretical study of orientation effects on flow boiling CHF," *Int. J. Heat Mass Transfer*, vol. 45, pp. 4463–4478, 2003.

[6] H. Zhang, I. Mudawar, and M. M. Hasan, "Flow boiling CHF in microgravity," *Int. J. Heat Mass Transfer*, vol. 48, pp. 3107–3118, 2005.

[7] H. Zhang, I. Mudawar, and M. M. Hasan, "Assessment of dimensionless CHF correlations for subcooled flow boiling in microgravity and earth gravity," *Int. J. Heat Mass Transfer*, vol. 50, pp. 4568–4580, 2007.

[8] R. J. Simoneau and F. F. Simon, "A visual study of velocity and buoyancy effects on boiling nitrogen," , , NASA Tech Note TN D-3354, 1966.

[9] K. Mishima and H. Nishihara, "The effect of flow direction and magnitude on CHF for low pressure water in thin rectangular channels," *Nucl. Eng. Design*, vol. 86, pp. 165–181, 1985.

[10] C. O. Gersey and I. Mudawar, "Effects of heater length and orientation on the trigger mechanism for near-saturated flow boiling CHF—I. Photographic and statistical characterization of the near-wall interfacial features," *Int. J. Heat Mass Transfer*, vol. 38, pp. 629–642, 1995.

[11] C. O. Gersey and I. Mudawar, "Effects of heater length and orientation on the trigger mechanism for near-saturated flow boiling CHF—II. CHF model," *Int. J. Heat Mass Transfer*, vol. 38, pp. 643–654, 1985.

[12] J. E. Galloway and I. Mudawar, "CHF mechanism in flow boiling from a short heated wall—Part 1. Examination of near-wall conditions with the aid of photomicrography and high-speed video imaging," *Int. J. Heat Mass Transfer*, vol. 36, pp. 2511–2526, 1993.

[13] J. E. Galloway and I. Mudawar, "CHF mechanism in flow boiling from a short heated wall—Part 2. Theoretical CHF model," *Int. J. Heat Mass Transfer*, vol. 36, pp. 2527–2540, 1993.

[14] M. Saito, N. Yamaoka, K. Miyazaki, M. Kinoshita, and Y. Abe, "Boiling two-phase flow under microgravity," *Nucl. Eng. Design*, vol. 146, pp. 451–461, 1994.

[15] T. H. Cochran, "Forced-convection boiling near inception in zero-gravity," , NASA Tech Note TN D-5612, 1970.

[16] Y. Ma and J. N. Chung, "A study of bubble dynamics in reduced gravity forced-convection boiling," *Int. J. Heat Mass Transfer*, vol. 44, pp. 399–415, 2001.

[17] Y. Ma and J. N. Chung, "An experimental study of critical heat flux (CHF) in microgravity forced-convection boiling," *Int. J. Multiphase Flow*, vol. 27, pp. 1753–1767, 2001.

[18] J. C. Sturgis and I. Mudawar, "Critical heat flux in a long, rectangular channel subjected to one-sided heating—I. Flow visualization," *Int. J. Heat Mass Transfer*, vol. 42, pp. 1835–1847, 1999.

[19] J. C. Sturgis and I. Mudawar, "Critical heat flux in a long, rectangular channel subjected to one-sided heating—II. Analysis of critical heat flux data," *Int. J. Heat Mass Transfer*, vol. 42, pp. 1849–1862, 1999.

[20] G. B. Wallis, *One-Dimensional Two-Phase Flow*. New York: McGraw-Hill, 1969.

Hui Zhang received the M.S. and Ph.D. degrees from Purdue University, West Lafayette, IN, in 2002 and 2006, respectively. His graduate work centered on the effects of reduced gravity on flow boiling heat transfer and critical heat flux.

He is currently a Postdoctoral Researcher at General Motors, Detroit, MI, investigating means to enhance the thermal performance of metal hydrides for automobile applications and measurement of thermal properties.

Issam Mudawar received the M.S. degree in 1980 and Ph.D. in 1984, both from the Massachusetts Institute of Technology, Cambridge. His graduate work involved magnetohydrodynamic (MHD) energy conversion and phase-change water cooling of turbine blades.

He joined the Purdue University School of Mechanical Engineering, West Lafayette, IN, in 1984, where he established, and became Director of, the Boiling and Two-Phase Flow Laboratory (BTPFL) and Purdue University International Electronic Alliance (PUIECA). His work has been focused on phase change processes, thermal management of electronic and aerospace devices, intelligent materials

processing, hydrogen storage, high-Mach turbine engines, and nuclear reactor safety. His theoretical and experimental research encompasses sensible and evaporative heating of thin films, pool boiling, flow boiling, jet-impingement cooling, spray cooling, micro-channel heat sinks, heat transfer enhancement, heat transfer in rotating systems, critical heat flux, and capillary pumped flows. He is also President of Mudawar Thermal Systems, Inc., a firm that is dedicated to the development of thermal management solutions.

Prof. Mudawar received several awards for his research accomplishments, including Best Paper Award in Electronic Cooling at the 1988 National Heat Transfer Conference, Best Paper Award in Thermal Management at the 1992 ASME/JSME Joint Conference on Electronic Packaging, the *Journal of Electronic Packaging* Outstanding Paper of the Year Award for 1995, and the Best Paper Award in Thermal Management at ITherm 2008. He also received several awards for excellence in teaching and service to Purdue students and their organizations, including the Solberg Award for Best Teacher in School of Mechanical Engineering (1987, 1992, 1996, 2004), the Charles Murphy Award for Best Teacher at Purdue University (1997), and the National Society of Black Engineers Professor of the Year Award (1985, 1987). He was named Fellow of the American Society of Mechanical Engineers (ASME) in 1998.

Mohammad M. Hasan received the M.S. and Ph.D. degrees from the University of Kentucky, Lexington, in 1978 and 1981, respectively. His graduate work involved natural convection heat transfer and critical heat flux in flow boiling.

He is a Research Scientist in the Fluid Physics and Transport Branch of the Space Experiment Division of the NASA Glenn Research Center, Cleveland, OH. He serves as Principal Investigator and Co-Investigator on various NASA projects related to fluid dynamics, heat and mass transfer in microgravity, and Advanced Thermal Control System (ATCS) development for space vehicles and space missions. His recent research is focused on the development of gravity-insensitive evaporator and condenser for the lunar heat pump, porous media condensing heat exchanger for crew cabin humidity control, phase change material heat exchanger for space vehicles/habitats, fluidized bed reactor for the lunar *in situ* resource utilization, and liquid oxygen storage and supply for exploration life support systems. He has performed extensive experimental and analytical investigations of fluid dynamics and heat and mass transfer problems related to in-space cryogenic fluid storage, conditioning, and pressure control. He was the Principal Investigator of the flight experiment "Tank Pressure Control Experiment: Thermal Phenomena," flown on the Space Shuttle STS-52 in 1992. Prior to joining NASA, he was an Assistant Professor in the Department of Mechanical and Aerospace Engineering of the University of Missouri-Rolla from 1982 to 1986.